Development of JNK2-Selective Peptide Inhibitors That Inhibit Breast Cancer Cell Migration

ARTICLE *in* ACS CHEMICAL BIOLOGY · MARCH 2011

Impact Factor: 5.33 · DOI: 10.1021/cb200017n · Source: PubMed

8 AUTHORS, INCLUDING:

Tamer Kaoud
University of Texas at Austin
48 PUBLICATIONS **314** CITATIONS
SEE PROFILE

Shreya Mitra
University of Texas MD Anderson Cancer Center
17 PUBLICATIONS **205** CITATIONS
SEE PROFILE

Michael A Cantrell
Stanford Medicine
9 PUBLICATIONS **98** CITATIONS
SEE PROFILE

Klaus Linse
Biosynthesis Inc.
23 PUBLICATIONS **418** CITATIONS
SEE PROFILE

Published in final edited form as:
ACS Chem Biol. 2011 June 17; 6(6): 658–666. doi:10.1021/cb200017n.

Development of JNK2-Selective Peptide Inhibitors that Inhibit Breast Cancer Cell Migration

Tamer S. Kaoud[§,¶], **Shreya Mitra**[§,#], **Sunbae Lee**[¶], **Juliana Taliaferro**[¶,‡], **Michael Cantrell**[†], **Klaus D. Linse**[¥], **Carla L. Van Den Berg**[*,†], and **Kevin N. Dalby**[*,¶]

[¶]Division of Medicinal Chemistry, College of Pharmacy, The University of Texas at Austin, Austin, TX-78712

[†]Division of Pharmacology and Toxicology, College of Pharmacy, The University of Texas at Austin, Austin, TX-78712

[‡]Pharm D Program, College of Pharmacy, The University of Texas at Austin, Austin, TX-78712

[¥]XBiotech USA Inc, Austin, TX-78744

[#]The University of Texas MD Anderson Cancer Center, Houston, TX 77030

Abstract

Despite their lack of selectivity towards c-Jun *N*-terminal kinase (JNK) isoforms, peptides derived from the JIP (JNK Interacting Protein) scaffolds linked to the cell-penetrating peptide TAT are widely used to investigate JNK-mediated signaling events. To engineer an isoform-selective peptide inhibitor, several JIP-based peptide sequences were designed and tested. A JIP sequence connected through a flexible linker to either the *N*-terminus of an inverted TAT sequence (JIP^{10}-Δ-TAT^{i}), or to a poly-arginine sequence (JIP^{10}-Δ-R_9) enabled the potent inhibition of JNK2 (IC_{50}~90 nM) and exhibited 10-fold selectivity for JNK2 over JNK1 and JNK3. Examination of both peptides in HEK293 cells revealed a potent ability to inhibit the induction of both JNK activation and c-Jun phosphorylation in cells treated with anisomycin. Notably, Western blot analysis indicates that only a fraction of total JNK must be activated to elicit robust c-Jun phosphorylation. To examine the potential of each peptide to selectively modulate JNK2 signaling *in vivo*, their ability to inhibit the migration of Polyoma Middle-T Antigen Mammary Tumor (PyVMT) cells was assessed. PyVMTjnk2-/- cells exhibit a lower migration potential compared to PyVMTjnk2+/+ cells, and this migration potential is restored through the over-expression of GFP-JNK2α. Both JIP^{10}-Δ-TAT^{i} and JIP^{10}-Δ-R_9 inhibit the migration of PyVMTjnk2+/+ cells and PyVMTjnk2-/- cells expressing GFP-JNK2α. However, neither peptide inhibits the migration of PyVMTjnk2-/- cells. A control form of JIP^{10}-Δ-TAT^{i} containing a single leucine to arginine mutation lacks ability to inhibit JNK2 *in vitro* cell-free and cell-based assays and does not inhibit the migration of PyVMTjnk2+/+ cells. Together, these data suggest that JIP^{10}-Δ-TAT^{i} and JIP^{10}-Δ-R_9 inhibit the migration of PyVMT cells through the selective inhibition of JNK2. Finally, the mechanism of inhibition of a D-*retro-inverso* JIP peptide, previously reported to inhibit JNK, was examined and found to inhibit p38MAPKα in an *in vitro* cell-free assay with little propensity to inhibit JNK isoforms.

INTRODUCTION

JNKs (c-Jun N-terminal kinases) are members of the mitogen-activated protein kinase (MAPK) family, which regulate various cellular functions (1). In response to stress, they can

[*]Correspondence should be addressed to K.N.D. (kinases@me.com) and C.V.B. (cvandenberg@mail.utexas.edu).
[§]Both authors contributed equally to this work.

convey pro-inflammatory, mitogenic or apoptotic signals (2). In mammals JNKs are encoded by three different genes (*jnk1, jnk2*, and *jnk3*), which may alternatively splice to produce a total of 10 different isoforms. The *jnk1* and *jnk2* genes are expressed ubiquitously, while JNK3 is expressed mainly in testes and neuronal tissues, including the brain with low levels also found in cardiac myocytes (3).

Jnk genes are implicated in several diseases such as type I and type II diabetes, Alzheimer's disease, arthritis, asthma, atherogenesis, heart failure and Parkinson's disease (4). Due to its important role in regulating both apoptosis and proliferation, JNK can act as a tumor-promoter and a tumor-suppressor in cancer (5, 6), both in a tissue and stimulus-specific manner. Overall, from the perspective of tumor biology, JNK mediates the transforming actions of oncogenes such as Ras and Bcr-Abl (7). A causal relationship between JNK activation and accelerated tumor growth has been reported in several studies (8) as the antisense JNK oligonucleotides were found to inhibit the growth of tumor cells (PC12, A549, HeLa, and MCF-7)(9).

Compared to *jnk1* and *jnk3*, the *jnk2* gene has a dominant role in cancer. For example, JNK2 is implicated in tumorigenesis via activation of Akt and over-expression of eukaryotic translation initiation factor 4 (eIF4E) in a human glioblastoma model (10). JNK2 is also constitutively activated in glial tumor cell lines, further supporting its tumorigenic role (11). Moreover, JNK2-knockout mice displayed lower growth of chemically-induced papillomas compared to wild type (12).

The Van Den Berg laboratory recently reported that JNK2 knockout mice expressing the Polyoma Middle T Antigen transgene developed mammary tumors showed higher tumor multiplicity but lower proliferation rates (13). Cell lines derived from these tumors provided useful tools to evaluate the potential function of JNK2 in various breast cancer phenotypes including cell migration (14).

Cell migration contributes to tissue repair and regeneration, mental retardation, atherosclerosis, arthritis, and embryonic morphogenesis (15), and migration is critically important in driving cancer metastasis. Mitogen activated protein kinases, including JNK, p38MAPKα and extracellular-signal-regulated protein kinase (ERK) play crucial roles in promoting cell migration (16). Biochemically, several JNK substrates such as IRS-1, p66Shc and paxillin promote cell migration (7). In fact, *jnk1* was implicated in embryonic epithelial cell migration by Weston et al., who showed a delay in eyelid closure resulting from corneal epithelial cell migration, in *jnk1-/-;jnk2+/-* mice compared to their *jnk1+/+;jnk2+/-* littermates (17).

Recent literature underscores the importance of JNKs as attractive targets for treatment of a variety of diseases, which has triggered extensive drug discovery efforts. In our investigation, our goal was to identify a JNK-specific inhibitor and, ideally, a JNK2 isoform-selective inhibitor that acts therapeutically to treat various JNK2-associated diseases, including cancer.

Due to the specificity limitations of most JNK inhibitors designed to bind in the ATP binding site, several groups have focused on identifying small molecule (18) or peptide inhibitors that bind to JIP-JNK interaction sites. For example, recently, the small molecule BI-78D3, which has an IC_{50} of 500 nM was reported (19). The JIP (**J**NK **I**nteracting **P**rotein) scaffolds, including JIP1, JIP2, JIP3 and JIP4, bind to both JNK and MKK7 and potentiate JNK activation. JIP1 is expressed in many tissue types, including neuronal, neuroendocrine, pulmonary, and renal, amongst others (20). JIP-based inhibitors have been developed through the use of the single D-domain (D-site) of JIP1, consisting of 11 amino

acids (153–163) that correspond to the JIP1 docking site of JNK. This 11-mer peptide (pepJIP1) acts as a specific inhibitor of JNK, which binds to inactive JNK1, as elucidated by crystallization, and functions through an allosteric inhibition mechanism (21). PepJIP1 inhibits JNK activity in *in vitro* cell-free assays towards recombinant c-Jun, Elk, and ATF2, and displays remarkable selectivity for the JNKs with little inhibition of the closely related MAPKs ERK and p38MAPKα (21).

While JNK1 inhibition by pepJIP1 occurs mainly through direct competition with a docking site (the D-site) of substrates or upstream kinases, allosteric effects may contribute to its potency and specificity. To increase cell permeability, pepJIP1 was fused with the HIV-TAT (Human Immuno-deficiency Virus-Trans-acting activator of transcription) peptide. Its administration in both genetically- and diet-induced mouse models of insulin resistance and Type 2 diabetes restores normoglycemia without causing hypoglycemia in lean mice (22). However, uncertainties remain regarding the specificity and selectivity towards different JNK isoforms for this group of peptides. Such characteristics potentially significantly affect their use as efficient therapeutic agents in targeting definitive active sites in the human body.

In this work, we investigated the role of JNK2 in cell migration and developed a JNK2-selective inhibitor that efficiently inhibits cell migration in a breast cancer cell line.

RESULTS AND DISCUSSION

Metastasis, the therapeutically elusive trait of cancer cells, is often regarded as an early event in tumor progression. It initiates through the up-regulation of motility genes, priming a specific pool of tumor cells to develop a migratory phenotype. These cells gain an adaptive advantage to respond to micro-environmental cues necessary to initiate proteolytic invasion of the surrounding matrix. Therefore, proteins involved in cancer cell migration are potential targets of anti-metastatic therapy. In this manuscript we describe two peptides with 10-fold selectivity for JNK2 over JNK1 and JNK3, which inhibit JNK docking interactions. These cell-permeable peptides inhibit the ability of cell lines derived from tumors arising from Polyoma Middle T Antigen (PyVMT) to undergo cell migration and support the notion that JNK2-selective inhibitors may be useful therapeutic targeting molecules against breast cancer metastasis.

Examining the specificity of JIP-based peptide inhibitors

The ability of JIP peptide inhibitors to selectively bind JNK1, 2 and 3 *versus* other MAPKs is well documented (21, 23, 24). However, an isoform specific JIP peptide inhibitor has not been reported. To explore the specificity of the JIP peptides a 10-mer $JIP_{144\text{-}153}$ peptide (JIP^{10}: PKRPTTLNLF) was synthesized and tested in *in vitro* kinase assays. This peptide is comprised of the amino acids 144–153 of JNK-binding domain of the JIP-1 scaffold protein. When tested in kinase assays, JIP^{10} inhibited the JNKs (Figure 1a), but did not show any selectivity towards the three JNK isoforms (Table 1a), which were inhibited with IC_{50}'s of 1.0–2.6 μM. As expected JIP^{10} exhibited a minimal ability to inhibit ERK2 (IC_{50} = 180 μM) and p38MAPKα (IC_{50} 168 μM). We reasoned that the absence of JNK isoform selectivity reflects the highly conserved nature of the D-recruiting site (DRS) of the JNKs, which binds the JIP^{10} sequence (25).

Cell penetrating peptides (CPP) have been used widely to deliver impermeable molecules into intact cells. A peptide from the TAT-HIV protein is one of the most frequently used CPPs (26). Thus, the arginine-rich domain of TAT, consisting of the amino acids 49–58 (TAT: GRKKRRQRRR), was employed to develop cell permeating JIP peptides. Using a cell penetrating peptide consisting of the $TAT_{48–58}$ sequence connected directly to the *N*-terminus of an 11-mer $JIP_{143–153}$ peptide (TAT-JIP^{10}: YGRKKRRQRRR-

RPKRPTTLNLF), Zhang, et al. demonstrated inhibition of JNK3 activation *in vivo*, resulting in neuronal protection against ischemic brain injury (27). When we tested this peptide in *in vitro* kinase assays, we found it displayed no isoform selectivity (Figure 1b), inhibiting JNK1, 2, and 3 with IC_{50} values of 1.1–1.9 μM (Table 1a). Thus, compared to JIP^{10} the *N*-terminal TAT sequence of TAT-JIP^{11} provides no additional selectivity amongst the JNK isoforms.

Bonny et al (2001) engineered a longer cell permeating peptide inhibitor of JNK by connecting the HIV-$TAT_{49–58}$ cell penetrating sequence to the *N*-terminus of the 20 amino acid inhibitory domain of JIP-1 (143–162). The two are joined by two proline residues, which act as a flexible linker between the TAT and the JIP sequences (28). We synthesized this peptide and tested its potency towards different MAP kinases in *in vitro* kinase assays. Interestingly, this peptide (TAT-*PP*-JIP^{20}: GRKKRRQRRR-*PP*-RPKRPTTLNLFPQVPRSQDT) exhibited a 5–7-fold selectivity for JNK3 over JNK1 and JNK2 with an IC_{50} of 60 nM for JNK3 (Figure 1d). However, we found that it inhibits p38MAPKα, JNK1 and JNK2 with similar potency (Figure 1c), with IC_{50}'s of 1.45 ± 0.1 μM, 0.33 ± 0.01 μM, and 0.5 ± 0.05 μM respectively (Table 1a).

Bonny et al (2001) also developed a cell-stable JIP-peptide composed of the D-retro-inverso form of TAT-*PP*-JIP^{20} (D-TAT-*PP*-JIP^{20}) (28). This peptide was proposed to have a beneficial effect on several neuronal disorders including cerebral ischemia (29), stroke, and Parkinson's disease (30), and was recently classified as a possible novel therapy for diabetes (22). All such effects were attributed to its inhibition of the JNK pathway in the cell, but the precise mechanism of neuroprotection remains unclear (31). Therefore the specificity of D-TAT-*PP*-JIP^{20} toward the three MAPK families was examined using the kinase assay described above. In addition, the isoform specificity of two reteroinverso peptides corresponding to residues 143–152 (D-JIP^{10}) and 143–162 (D-JIP^{20}) were examined. D-JIP^{10} and D-JIP^{20} showed negligible inhibition towards the five MAP kinases tested (Table 1b). Recently we studied the specificity of a docking interaction between JNK1 and the scaffolding protein JIP1 (25). Free energies for the binding of JIP^{10} and D-JIP^{10} were estimated using molecular mechanics Poisson-Boltzmann and Generalized-Born surface area (MM-PB/GBSA) methods. The binding free energy calculations predicted that the binding of the JIP (D) form (D-JIP^{10}) to JNK1 is significantly weaker than the binding of the JIP (L) form (JIP^{10}). This was also confirmed experimentally (25).

Interestingly, D-TAT-*PP*-JIP^{20} exhibited a moderate ability to inhibit JNK3 (IC_{50} ~ 76 μM), with a potency 4–5 times higher than JNK1 and JNK2 (IC_{50} 290 ± 25 μM and 350 ± 80 μM respectively) (Figure 2a). Surprisingly, it exhibits even greater potency towards p38MAPKα (Figure 2a). Thus, D-TAT-*PP*-JIP^{20} fully inhibits the phosphorylation of a peptide substrate by p38MAPKα with an IC_{50} of 1.8 ± 0.18 μM and can inhibit the phosphorylation of GST-ATF2 (Δ1–115) by p38MAPKα with an IC_{50} of 14 ± 0.1 μM (Figure 2b). These data suggest that p38MAPKα (and not the JNKs) is a potential target of D-TAT-*PP*-JIP^{20} *in vivo*.

Taken together, the studies described above suggest that the extension of peptides beyond the DRS docking domain can lead to changes in selectivity and potency. Therefore, we decided to engineer a new generation of cell penetrating JIP-based peptides. In doing so, we changed the position of the TAT peptide relative to the JIP sequence and introduced a flexible linker that connects the JIP and CP domains together. After testing several designed sequences, we developed a peptide with significant selectivity for JNK2. The backbone of this peptide consists of the 10 mer $JIP_{144–153}$ peptide connected to the *N*-terminus of an inverted HIV-$TAT_{49–58}$ sequence through a flexible six carbon linker formed by a 6-aminohexanoyl group (JIP^{10}-Δ- TAT^{i}: PKRPTTLNLF-Δ-RRRQRRKKRG). JIP^{10}-Δ-TAT^{i} inhibits JNK2, with an IC_{50} of 92 nM (Figure 3a) exhibiting a 10 to 12-fold selectivity over

JNK1 (IC_{50} = 1.2 ± 0.05 μM) and JNK3 (IC_{50} of 1.2 ± 0.07 μM) (Table 1a). Moreover, JIP^{10}-Δ-TAT^i did not exhibit marked potency towards p38MAPKα or ERK2 (Figure 3b). Similarly, we developed another peptide with the same backbone as JIP^{10}-Δ-TAT^i, but instead used nine arginine residues in place of the TAT sequence to enhance the cell penetration (JIP^{10}-Δ-R^9: PKRPTTLNLF-Δ-RRRRRRRRR). JIP^{10}-Δ-R^9 exhibited a similar selectivity to JIP^{10}-Δ-TAT^i, with high potency towards JNK2 (IC_{50} = 89 nM) (Figure 3c and d).

JIP^{10}-Δ-TAT^i and JIP^{10}-Δ-R^9 are efficient cell penetrating peptides

Before testing the *in vivo* bioactivity of the developed peptides, we investigated whether these peptides can be translocated efficiently into breast cancer cells. To do so, each peptide was labeled at its *C*-terminus on a Cys residue with FITC (Fluorescein isothiocyanate dye). *In vivo* localization of JIP^{10}-Δ-TAT^i and JIP^{10}-Δ-R^9 was accomplished using either 4T1.2 murine mammary cancer cells treated with 2 μM of FITC labeled JIP^{10}-Δ-TAT^i (FITC-JIP^{10}-Δ-TAT^i) or PyVMT murine mammary cancer cells treated with 2 μM of FITC labeled peptides (FITC-JIP^{10}-Δ-TAT^i or FITC-JIP^{10}-Δ-R^9).

Live cell images were captured of highly metastatic 4T1.2 murine mammary carcinoma cells (Figure 4a) revealing that the FITC- JIP^{10}-Δ-TAT^i peptide efficiently penetrated into the cytoplasm and nucleus within 30 minutes of incubation. The case was similar for PyVMT cells, as both labeled peptides (FITC-JIP^{10}-Δ-TAT^i or FITC-JIP^{10}-Δ-R^9) could rapidly enter PyVMT cells once added to the culture medium. Figure 4b shows images of live PyVMT cells captured after 15 and 60 minutes of peptide treatment. Notably, although these peptides rapidly penetrate into the cytoplasm of PyVMT cells within minutes of addition to the culture medium, their entrance into the nucleus requires up to an hour.

Effects of peptides on JNK activation and c-Jun phosphorylation in HEK293T cells

JIP peptides are known to work as JNK inhibitors by acting as a barrier to the interaction of JNKs with the upstream kinases MKK4 and MKK7 and downstream substrates e.g c-Jun (21). Western blot analysis was employed to examine the effect of peptide treatment (5–100 μM, 16 hours) on the activation of JNK or the phosphorylation of c-Jun, following stimulation of JNK by anisomycin (Figure 5). Phosphorylation of c-Jun, an *in vivo* substrate of the JNKs (31) is strongly inhibited by both JIP^{10}-Δ-TAT^i and JIP^{10}-Δ-R^9 in cell-free *in vitro* assays (Figure 3). The Western blot analysis reveals that the incubation of HEK293T cells with either peptide leads to a dose-dependent decrease in c-Jun phosphorylation. 5 μM of either peptide results in more than a 50% inhibition of c-Jun phosphorylation and 95% inhibition was achieved at higher concentrations (c.a. 100 μM) (Figure 5). Interestingly, 5 μM of either peptide was enough to inhibit the activation/phosphorylation of cellular JNKs by ~ 90 % and the inhibitory potency of JIP^{10}-Δ-R^9 was clearly higher than JIP^{10}-Δ-TAT^i especially at concentrations ≥ 10 μM. As a control, cells were incubated with *m*JIP^{10}-Δ-TAT^i, which has the same sequence as JIP^{10}-Δ-TAT^i except for a single point mutation (L150R) in $JIP_{144–153}$, which renders it incapable of inhibiting any of the MAP kinases tested (Table 1a). As shown in Figure 5, 100 μM JIP^{10}-Δ-TAT^i inhibits neither JNK activation nor c-Jun phosphorylation, strongly supporting the notion that JIP^{10}-Δ-TAT^i and JIP^{10}-Δ-R^9 directly bind JNKs and prevent their interactions with upstream and downstream protein targets. These studies demonstrate the efficacy of both peptides in a cell-based system and reveal that only a fraction of total JNK must be activated to elicit robust signaling to a downstream substrate.

Assessing JNK2-specific peptides in breast cancer cells

To date a cellular assay specific for endogenous JNK2 has not been developed. Recently, however the Van Den Berg laboratory revealed a specific role for JNK2 in mammary cancer

cell migration using the PyVMT model of mammary tumorigenesis (13). The PyVMT model is important due to its close resemblance to the actual human disease both in tumor progression stages and in genetic alterations: notably Src, Shc, and PI3K signaling are upregulated in the PyVMT model, and their signaling is also often upregulated in human breast tumors (13). Cell lines derived from PyVMT jnk2+/+ or jnk2-/- tumors were verified with respect to JNK2 expression by both qPCR and Western blotting (14). Furthermore, JNK1α 1/2 (p55), JNK1β2 (p46) and JNK3 were shown to be expressed similarly in both cell lines (14).

We utilized a recent observation, that the migration potential of PyVMTjnk2+/+ cells is reproducibly five-fold greater than that of PyVMTjnk2-/- cells (14). This observation provided a JNK2 specific functional assay with which to test the inhibitor, since the exogenous expression of GFP-JNK2α in the PyVMTjnk2-/- cells significantly restored the ability of the cells to migrate (14).

Therefore, we examined whether JIP^{10}-Δ-TAT^{i} and JIP^{10}-Δ-R_9 inhibited directional breast cancer cell migration in these PyVMT cell lines. As a control we also utilized *m*JIP^{10}-Δ-TAT^{i}. Thus, PyVMTjnk2+/+ cells were treated with no peptide, *m*JIP^{10}-Δ-TAT^{i} (10 μM) as a negative control, JIP^{10}-Δ-TAT^{i} (10 μM), and JIP^{10}-Δ-R_9 (10 μM) (Figure 6). Cell viability was monitored during the migration assay and found to be unaffected by the addition of the peptides (data not shown). Untreated PyVMTjnk2+/+ cells showed robust migration, similar to those treated with the mutant peptide *m*JIP^{10}-Δ-TAT^{i}. In contrast, the JIP^{10}-Δ-TAT^{i} and especially JIP^{10}-Δ-R_9 displayed a strong inhibition of cell migration. These data are consistent with the observed potency of the peptides towards JNK2 in both cell free (Table 1) and cell-based *in vitro* assays (Figure 5).

To further confirm the activity of the newly engineered peptides towards JNK2 *in vivo*, we used PyVMTjnk2-/- cells expressing GFP or GFP-JNK2α2 and tested their ability to migrate when treated with *m*JIP^{10}-Δ-TAT^{i} (10 μM), JIP^{10}-Δ-TAT^{i} (10 μM), or JIP^{10}-Δ-R_9 (10 μM). None of the peptides affected the migration of PyVMTjnk2-/- cells expressing GFP alone indicating that the absence of JNK2α in these cells renders JNK2-selective peptides ineffective with respect to the further inhibition of cell migration (Figure 7a and 7b).

However, the exogenous-expression of GFP-JNK2α2 in PyVMTjnk2-/- cells, which restores the capacity of PyVMTjnk2-/- cells to migrate, once again sensitized them to the JNK2-selective peptides. Thus, while the mutant peptide *m*JIP^{10}-Δ-TAT^{i} (10 μM) had no effect on the migration of PyVMTjnk2-/-GFP-JNK2α2 cell migration the JNK2-selective peptides JIP^{10}-Δ-TAT^{i} and JIP^{10}-Δ-R_9 both inhibited migration (Figure 7a and 7b).

To summarize, recently the Van Den Berg laboratory demonstrated that knockout of JNK2 inhibits migration of murine mammary carcinoma cells. Accordingly, the cell permeable JNK2-selective peptide inhibitors (JIP^{10}-Δ-TAT^{i} and JIP^{10}-Δ-R_9) reduced PyVMTjnk2+/+ cell migration to a level similar to the migration of PyVMTjnk2-/- cells. Compared to previously developed peptide inhibitors, JIP^{10}-Δ-TAT^{i} and JIP^{10}-Δ-R_9 were more potent and selective towards JNK2 in *in vitro* kinase assays. Finally, with regards to the mechanism of inhibition of previously reported D-retro-inverso JIP peptides, the most widely used D-TAT-$_{pp}$-JIP^{20} showed an unexpected level of potency towards p38MAPKα and little activity towards any JNK isoform.

METHODS

Cell culture

Mouse mammary tumor cell lines were derived from PyVMTjnk2+/+ and PyVMTjnk2-/- tumors using a previously published protocol (13). PyVMT jnk2-/- cells stably expressing GFP- JNK2α2, PyVMT jnk2-/- GFP- JNK2α2, were generated following selection with puromycin. Cells were maintained in DMEM F-12 media (Cellgro, Mediatech) with 10% (v/v) FBS (Gemini Bio-Products), 10 μg mL^{-1} insulin (Humulin R™), 5 ng mL^{-1} EGF (PeproTech), and antibiotics. For experiments using JIP peptides, cells were pre-incubated with various peptides for 30 minutes prior to assaying for migration. The JIP peptides were maintained in the culture media for the duration of the experiment.

HEK293T cells were maintained in DMEM (Invitrogen) supplemented with 10% (v/v) FBS-US grade (Invitrogen), 2 mM L-glutamine (Invitrogen), 100 U mL^{-1} penicillin (Sigma), and 100 g mL^{-1} streptomycin (Sigma). Cells were cultured in a humidified 5% CO_2 incubator at 37 °C. Cells were seeded at 400,000 cells per well in a 12-well plate and incubated for 24 hours before incubation with or without peptide (32). After 16 hours cells were treated with anisomycin (50–100 nM) (MP Biomedicals) for 5–10 minutes.

Western blot analysis

Cells were washed in PBS (Invitrogen), and lysates were prepared in CytoBuster™ Protein Extraction Reagent (EMD-Biosciences). The lysates were cleared by centrifugation, and the protein concentration measured by Bradford analysis (Bio-Rad). Lysates containing 60 μg of total protein were fractionated on a 12% SDS polyacrylamide gel (Bio-Rad) and transferred to Hybond-P PVDF Membrane (GE Healthcare). Incubation of primary antibodies was performed overnight at 4 °C using 1:10,000 anti-phospho-c-Jun (Ser-63), clone Y172 rabbit mAb (Millipore); 1:2000 anti-phospho-SAPK/JNK (Thr183/Tyr185) (G9) mouse mAb (Cell Signaling Technology); 1:5000 anti-actin, clone 4 mouse mAb (Millipore). Either anti-mouse (Cell Signaling Technology) or anti-rabbit (Bio-Rad) horseradish peroxidase-conjugated secondary antibodies and ECL Plus™ Western Blotting Reagents (GE Healthcare) were used to develop the blots.

Cell migration

Cell migration was measured using a modified Boyden chamber (BD Biosciences). About 50, 000 cells were placed into the upper chamber of transwell chambers separated by inserts with 8 μm pores. Lower chambers were filled with HBSS (Hank's Buffered Salt Solution) medium containing 1% (v/v) FBS as chemoattractant. Cells were allowed to migrate for 8 hrs. Migrated cells were fixed, stained with 0.5% (w/v) crystal violet, and quantified by counting four randomly chosen fields (at an objective of ×10), or by dissolving the crystal violet dye with sodium citrate and reading the absorbance (blank adjusted) at 570 nm.

JIP internalization

About 50, 000 cells were plated in 8-well chamber slides. The next day, slides were kept on ice for 10 minutes to stall all cellular activity and uptake. FITC-labeled JIP peptides at 10 μM were added to the medium at 37 °C and incubated for various amounts of time. The cell nucleus was briefly stained with Hoechst dye and then the cells imaged in real time. The fluorescent signal was detected using a CCD camera mounted on a Nikon Diaphot 300 inverted microscope.

Statistics

Results were evaluated using analysis of variance between groups, followed by non-parametric, post-hoc Student's t-test to identify differences between groups. Differences between means yielding p values of ≤ 0.05 were considered statistically significant.

MAP kinase activity assay

MAP kinase assays were conducted at 30 °C in kinase assay buffer (25 mM HEPES buffer-pH 7.5, 50 mM KCl, 0.1 mM EDTA, 0.1 mM EGTA, 2 mM DTT and 10 μg mL^{-1} BSA), containing 500 μM [γ-^{32}P] ATP (100-1000 c.p.m. $pmol^{-1}$), 11 mM $MgCl_2$ and different concentrations of the JIP peptides in a final total volume of 70 μL. *For JNK assays*, 20 nM active JNK1α1, JNK2α2 or JNK3α2 were assayed with 2 μM GST-c-jun (1–221) as protein substrate. *For p38MAPKα assays*, 10 nM p38MAPKα was assayed with either 10 μM of a substrate peptide (FQRKTLQRRLKGLNLNL-AHX-TGPLSPGPF, where AHX is a linker), which has a specific D-site to the MAP kinases (described in Lee et al., *in preparation*) or 10 μM GST-ATF2 (1–115) protein substrate. *For ERK2 assays* 2 nM ERK2 was assayed with 10 μM of the Dsite substrate peptide. Activity was assessed at different peptide concentrations by the measurement of initial rates. Rates were measured under conditions where the total product formation represented less than 10% of the initial substrate concentrations. The reaction was initiated by the addition of ATP. 10 μL aliquots were taken from every reaction at set time points (0.5, 1, 1.5, 2, 4 min) and spotted to 2×2 cm^2 squares of P81 cellulose paper; the papers were washed for 3×15 minutes in 50 mM phosphoric acid (H_3PO_4), followed by a pure acetone wash, then dried. The amount of labeled protein was determined by counting the associated c.p.m. on a Packard 1500 scintillation counter at a sigma value of 2.

Peptide synthesis and purification

D- and L-peptides were synthesized and purified using the same method described by Yan C. et al (25). Peptides were synthesized on rink resin (NovaSyn TGR resin) using a Peptide Synthesizer (Quartet, Rainin) utilizing an Fmoc solid-phase peptide synthesis protocol. The optical rotation of each Fmoc-D amino acid was examined to confirm their chirality by utilizing a polarimeter (241MC Polarimeter, Perkin-Elmer).

Expression, purification and activation of tagless MAPKs

Tagless full length human JNK1α1 (GenBank accession number NM_002750), human JNK2α2 (GenBank accession number NM_002752) or *N*-terminal truncated human JNK3α2 (amino acids 39–422 with alanine inserted between amino acids 39 and 40, GenBank accession number NM_138982) were expressed and purified as described previously (25, 33). Activated tagless ERK2 (Rattus norvegicus mitogen activated protein kinase 1, GenBank accession number NM_053842) was expressed and purified as described elsewhere (Kaoud et al. *manuscript submitted*). DNA sequences encoding Mus musculus mitogen-activated protein kinase 14 - p38MAPKα (GenBank accession number NM_011951) was cloned into the pET14B vector to express an *N*-terminal, His tagged p38MAPKα in E. coli BL21 (DE3) pLysS cells. The enzyme was expressed and purified as described previously (34). The activated, MAPKs were all stored in buffer S [25 mM HEPES (pH 7.5), 50 mM KCl, 0.1 mM EDTA, 0.1 mM EGTA, 2 mM DTT and 10% (v/v) glycerol] at -80 °C.

Expression, purification of GST-c-Jun (1–221) and GST-ATF2 (1–115)

GST-c-Jun (1–221) was expressed and purified according to the method of Yan C. et al (25). GST-ATF2 (1–115) was expressed and purified according to the method of Szafranska et al. (34).

Acknowledgments

Financial support was from grants from the National Institute of General Medical Sciences (GM 059802), the Welch Foundation (F-1390) to K.N.D and NIH (CA 100238) to C.L.V.D.B.. Support from Texas Institute for Drug & Diagnostic Development H-F-0032 is also acknowledged. The content is solely the responsibility of the authors and does not necessarily represent the official views of the National Institute of General Medical Sciences or the National Institutes of Health. T.S.K. acknowledges a scholarship from the Egyptian Ministry of Higher Education. The table of content figure was produced by Dr. A. Syrett. The authors wish to thank Dr. Bulent Ozpolat for a critical review of an early draft of the manuscript.

References

1. Davis RJ. Signal transduction by the JNK group of MAP kinases. Cell. 2000; 103:239–252. [PubMed: 11057897]
2. Manning AM, Davis RJ. Targeting JNK for therapeutic benefit: from junk to gold? Nat Rev Drug Discov. 2003; 2:554–565. [PubMed: 12815381]
3. Gupta S, Barrett T, Whitmarsh AJ, Cavanagh J, Sluss HK, Derijard B, Davis RJ. Selective interaction of JNK protein kinase isoforms with transcription factors. EMBO J. 1996; 15:2760–2770. [PubMed: 8654373]
4. Bogoyevitch MA, Ngoei KR, Zhao TT, Yeap YY, Ng DC. c-Jun N-terminal kinase (JNK) signaling: recent advances and challenges. Biochim Biophys Acta. 1804:463–475. [PubMed: 19900593]
5. Kennedy NJ, Davis RJ. Role of JNK in tumor development. Cell Cycle. 2003; 2:199–201. [PubMed: 12734425]
6. Shibata W, Maeda S, Hikiba Y, Yanai A, Sakamoto K, Nakagawa H, Ogura K, Karin M, Omata M. c-Jun NH2-terminal kinase 1 is a critical regulator for the development of gastric cancer in mice. Cancer Res. 2008; 68:5031–5039. [PubMed: 18593901]
7. Bogoyevitch MA, Kobe B. Uses for JNK: the many and varied substrates of the c-Jun N-terminal kinases. Microbiol Mol Biol Rev. 2006; 70:1061–1095. [PubMed: 17158707]
8. Igaki T, Pagliarini RA, Xu T. Loss of cell polarity drives tumor growth and invasion through JNK activation in Drosophila. Curr Biol. 2006; 16:1139–1146. [PubMed: 16753569]
9. Potapova O, Anisimov SV, Gorospe M, Dougherty RH, Gaarde WA, Boheler KR, Holbrook NJ. Targets of c-Jun NH(2)-terminal kinase 2-mediated tumor growth regulation revealed by serial analysis of gene expression. Cancer Res. 2002; 62:3257–3263. [PubMed: 12036942]
10. Antonyak MA, Kenyon LC, Godwin AK, James DC, Emlet DR, Okamoto I, Tnani M, Holgado-Madruga M, Moscatello DK, Wong AJ. Elevated JNK activation contributes to the pathogenesis of human brain tumors. Oncogene. 2002; 21:5038–5046. [PubMed: 12140754]
11. Tsuiki H, Tnani M, Okamoto I, Kenyon LC, Emlet DR, Holgado-Madruga M, Lanham IS, Joynes CJ, Vo KT, Wong AJ. Constitutively active forms of c-Jun NH2-terminal kinase are expressed in primary glial tumors. Cancer Res. 2003; 63:250–255. [PubMed: 12517805]
12. Chen N, Nomura M, She QB, Ma WY, Bode AM, Wang L, Flavell RA, Dong Z. Suppression of skin tumorigenesis in c-Jun NH(2)-terminal kinase-2-deficient mice. Cancer Res. 2001; 61:3908–3912. [PubMed: 11358804]
13. Chen P, O'Neal JF, Ebelt ND, Cantrell MA, Mitra S, Nasrazadani A, Vandenbroek TL, Heasley LE, Van Den Berg CL. Jnk2 effects on tumor development, genetic instability and replicative stress in an oncogene-driven mouse mammary tumor model. PLoS One. 2010; 5:e10443. [PubMed: 20454618]
14. Mitra S, Lee JS, Cantrell M, Van Den Berg CL. cJun N-terminal kinase 2 (JNK2) enhances cell migration through epidermal growth factor substrate 8 (EPS8). The Journal of Biological Chemistry. 2011 in press.
15. Ridley AJ, Schwartz MA, Burridge K, Firtel RA, Ginsberg MH, Borisy G, Parsons JT, Horwitz AR. Cell migration: integrating signals from front to back. Science. 2003; 302:1704–1709. [PubMed: 14657486]
16. Huang C, Jacobson K, Schaller MD. MAP kinases and cell migration. J Cell Sci. 2004; 117:4619–4628. [PubMed: 15371522]

17. Weston CR, Davis RJ. The JNK signal transduction pathway. Curr Opin Cell Biol. 2007; 19:142–149. [PubMed: 17303404]

18. Chen T, Kablaoui N, Little J, Timofeevski S, Tschantz WR, Chen P, Feng J, Charlton M, Stanton R, Bauer P. Identification of small-molecule inhibitors of the JIP-JNK interaction. Biochem J. 2009; 420:283–294. [PubMed: 19243309]

19. Stebbins JL, De SK, Machleidt T, Becattini B, Vazquez J, Kuntzen C, Chen LH, Cellitti JF, Riel-Mehan M, Emdadi A, Solinas G, Karin M, Pellecchia M. Identification of a new JNK inhibitor targeting the JNK-JIP interaction site. Proc Natl Acad Sci U S A. 2008; 105:16809–16813. [PubMed: 18922779]

20. Whitmarsh AJ, Kuan CY, Kennedy NJ, Kelkar N, Haydar TF, Mordes JP, Appel M, Rossini AA, Jones SN, Flavell RA, Rakic P, Davis RJ. Requirement of the JIP1 scaffold protein for stress-induced JNK activation. Genes Dev. 2001; 15:2421–2432. [PubMed: 11562351]

21. Heo YS, Kim SK, Seo CI, Kim YK, Sung BJ, Lee HS, Lee JI, Park SY, Kim JH, Hwang KY, Hyun YL, Jeon YH, Ro S, Cho JM, Lee TG, Yang CH. Structural basis for the selective inhibition of JNK1 by the scaffolding protein JIP1 and SP600125. EMBO J. 2004; 23:2185–2195. [PubMed: 15141161]

22. Kaneto H, Nakatani Y, Miyatsuka T, Kawamori D, Matsuoka TA, Matsuhisa M, Kajimoto Y, Ichijo H, Yamasaki Y, Hori M. Possible novel therapy for diabetes with cell-permeable JNK-inhibitory peptide. Nat Med. 2004; 10:1128–1132. [PubMed: 15448687]

23. Barr RK, Kendrick TS, Bogoyevitch MA. Identification of the critical features of a small peptide inhibitor of JNK activity. J Biol Chem. 2002; 277:10987–10997. [PubMed: 11790767]

24. Barr RK, Boehm I, Attwood PV, Watt PM, Bogoyevitch MA. The critical features and the mechanism of inhibition of a kinase interaction motif-based peptide inhibitor of JNK. J Biol Chem. 2004; 279:36327–36338. [PubMed: 15208323]

25. Yan C, Kaoud TS, Lee S, Dalby KN, Ren P. Understanding the Specificity of a Docking Interaction between JNK1 and the Scaffolding Protein JIP1. The Journal of Physical Chemistry B. 2010 In press.

26. Ekokoski E, Aitio O, Tornquist K, Yli-Kauhaluoma J, Tuominen RK. HIV-1 Tat-peptide inhibits protein kinase C and protein kinase A through substrate competition. Eur J Pharm Sci. 2010; 40:404–411. [PubMed: 20433920]

27. Guan QH, Pei DS, Zong YY, Xu TL, Zhang GY. Neuroprotection against ischemic brain injury by a small peptide inhibitor of c-Jun N-terminal kinase (JNK) via nuclear and non-nuclear pathways. Neuroscience. 2006; 139:609–627. [PubMed: 16504411]

28. Bonny C, Oberson A, Negri S, Sauser C, Schorderet DF. Cell-permeable peptide inhibitors of JNK: novel blockers of beta-cell death. Diabetes. 2001; 50:77–82. [PubMed: 11147798]

29. Borsello T, Clarke PG, Hirt L, Vercelli A, Repici M, Schorderet DF, Bogousslavsky J, Bonny C. A peptide inhibitor of c-Jun N-terminal kinase protects against excitotoxicity and cerebral ischemia. Nat Med. 2003; 9:1180–1186. [PubMed: 12937412]

30. Kuan CY, Burke RE. Targeting the JNK signaling pathway for stroke and Parkinson's diseases therapy. Curr Drug Targets CNS Neurol Disord. 2005; 4:63–67. [PubMed: 15723614]

31. Repici M, Mare L, Colombo A, Ploia C, Sclip A, Bonny C, Nicod P, Salmona M, Borsello T. c-Jun N-terminal kinase binding domain-dependent phosphorylation of mitogen-activated protein kinase kinase 4 and mitogen-activated protein kinase kinase 7 and balancing cross-talk between c-Jun N-terminal kinase and extracellular signal-regulated kinase pathways in cortical neurons. Neuroscience. 2009; 159:94–103. [PubMed: 19135136]

32. Renlund N, Pieretti-Vanmarcke R, O'Neill FH, Zhang L, Donahoe PK, Teixeira J. c-Jun N-terminal kinase inhibitor II (SP600125) activates Mullerian inhibiting substance type II receptor-mediated signal transduction. Endocrinology. 2008; 149:108–115. [PubMed: 17947357]

33. Madsen JA, Kaoud TS, Dalby KN, Brodbelt JS. 193-nm photodissociation of singly and multiply charged peptide anions for acidic proteome characterization. Proteomics. 2011

34. Szafranska AE, Luo X, Dalby KN. Following in vitro activation of mitogen-activated protein kinases by mass spectrometry and tryptic peptide analysis: purifying fully activated p38 mitogen-activated protein kinase alpha. Anal Biochem. 2005; 336:1–10. [PubMed: 15582552]

35. Morrison JF. Kinetics of the reversible inhibition of enzyme-catalysed reactions by tight-binding inhibitors. Biochim Biophys Acta. 1969; 185:269–286. [PubMed: 4980133]

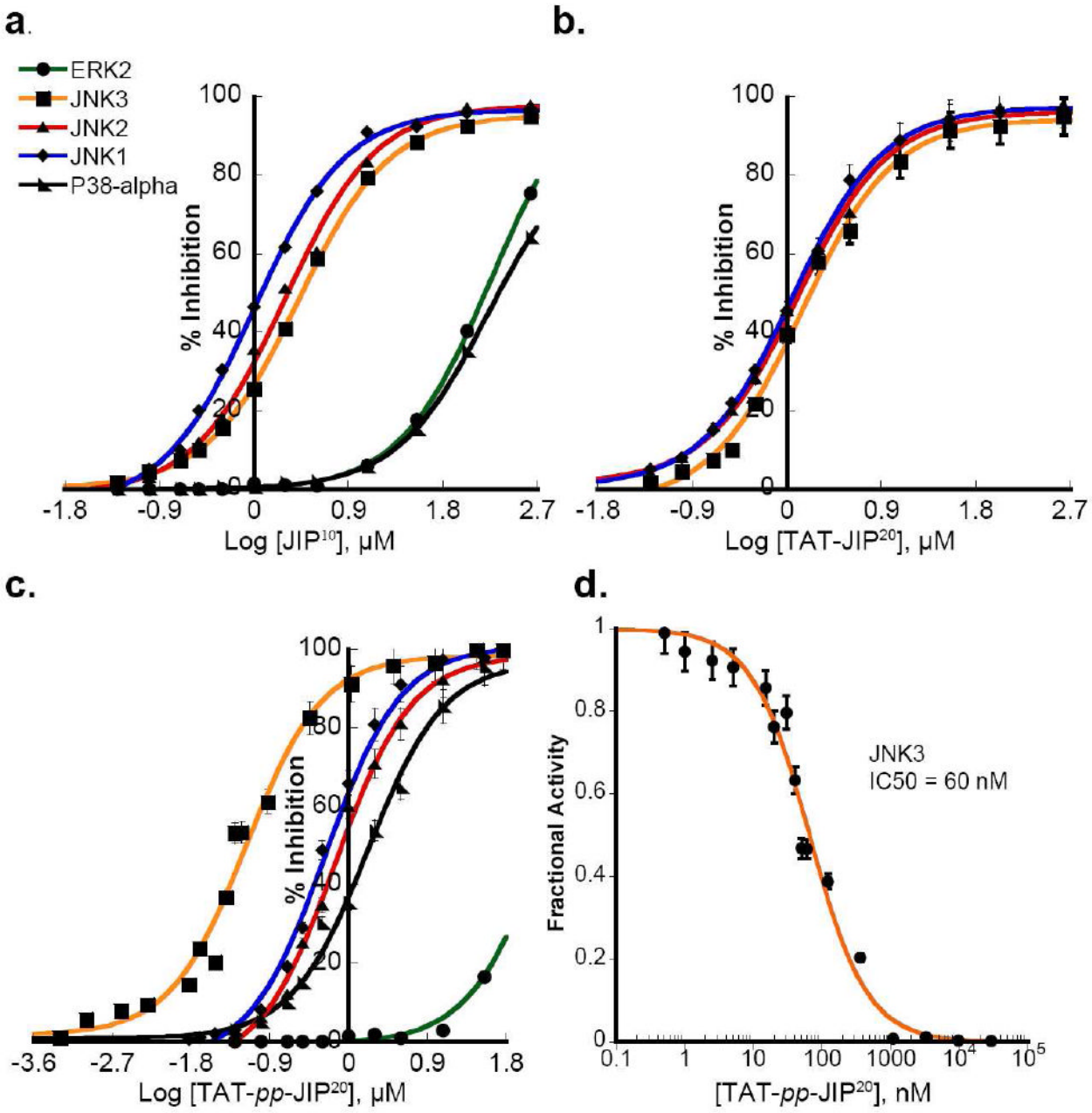

Figure 1. Selectivity of previously reported JIP peptides

The effect of peptides on the ability of JNKs to phosphorylate GST-c-JUN (1–221) and p38MAPKα or ERK2 to phosphorylate a peptide substrate was tested. a) JIP^{10} is non-selective towards specific JNK isoforms. b) The cell permeable peptide TAT-JIP^{10} does not show selectivity towards any of the three JNK isoforms. c) The cell permeable peptide TAT-*pp*-JIP^{20} exhibits five-fold greater selectivity for JNK3 over JNK1 and JNK2, but inhibits p38MAPKα, JNK1 and JNK2 with similar potency. d) TAT-*pp*-JIP^{20} exhibits marked potency towards JNK3, with an IC_{50} ~ 60 nM, as determined by fitting the fractional activity at every inhibitor concentration to Morrison's equation for a tight-binding inhibitor (35).

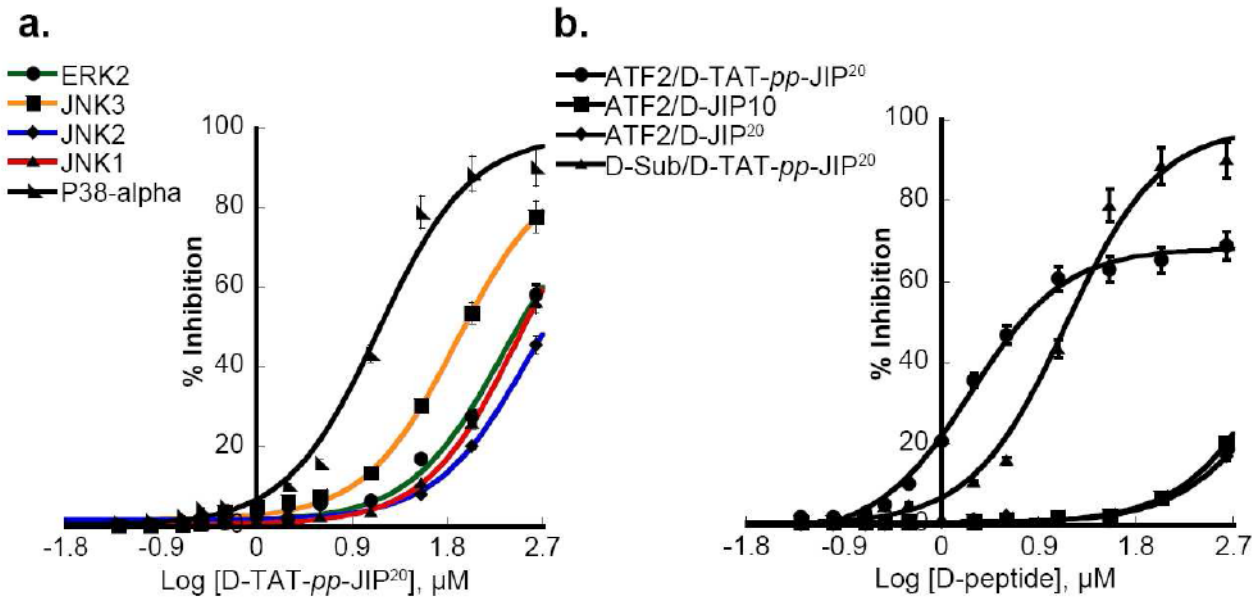

Figure 2. Selectivity of *retro-inverso* forms of JIP peptide

a) The effect of the cell permeable peptide D-TAT-*pp*-JIP^{20} on the ability of JNK to phosphorylate GST-c-JUN (1–221) and of p38MAPKα and ERK2 to phosphorylate a peptide substrate was examined. D-TAT-*pp*-JIP^{20} is a moderately more potent inhibitor of p38MAPKα than the three JNK isoforms. D-TAT-*pp*-JIP^{20} weakly inhibits JNK3, and marginally inhibits JNK1, JNK2 and ERK2. b) The phosphorylation of 10 μM GST-ATF2 (1–115) by p38MAPKα is not affected by D-JIP^{10} or D-JIP^{20}, while D-TAT-*pp*-JIP^{20} diminishes the ability of p38MAPKα to phosphorylate GST-ATF2 (IC_{50} ~ 1.9 μM), and the peptide substrate (IC_{50}~14 μM).

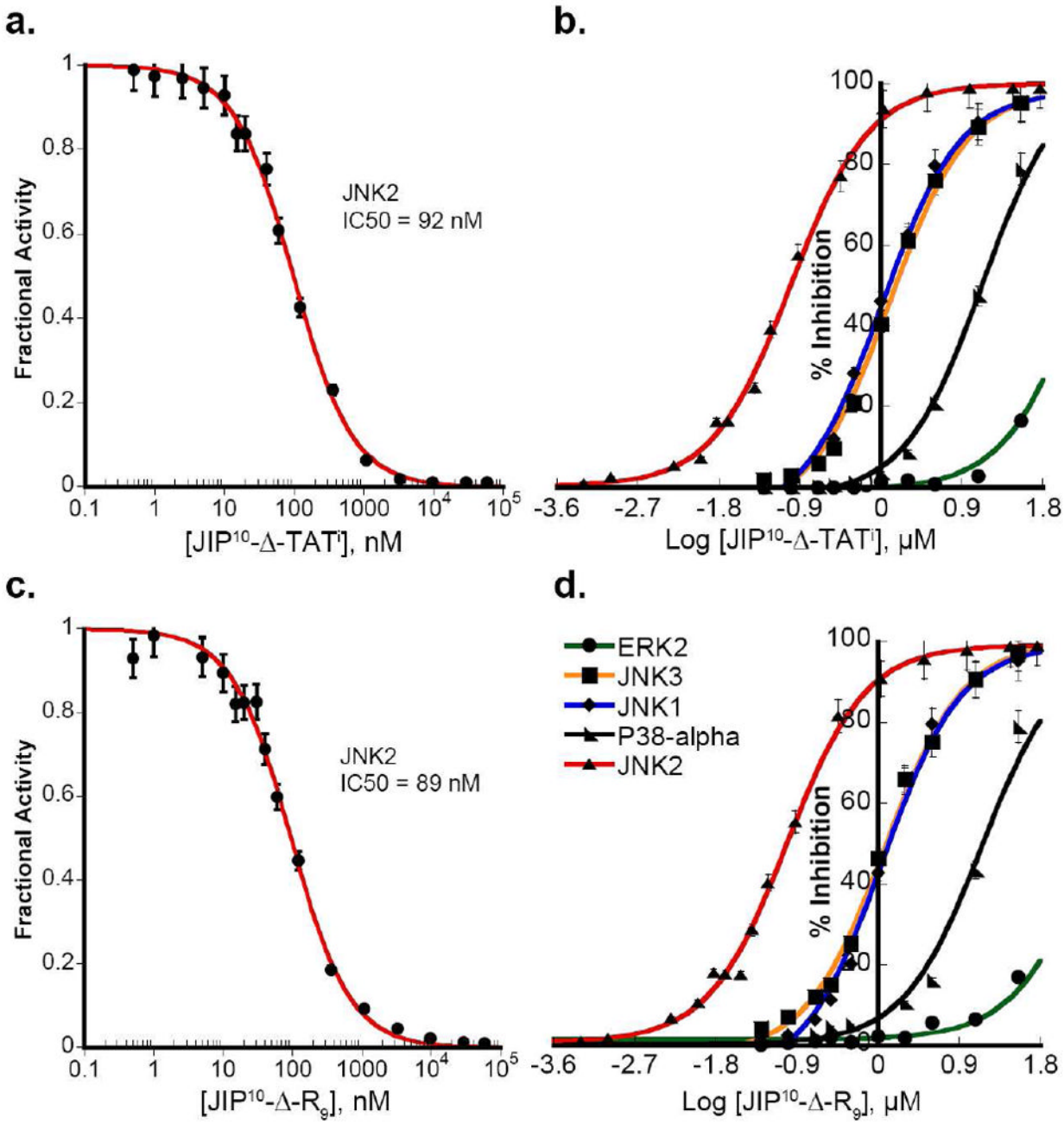

Figure 3. Selectivity of newly engineered peptide inhibitors towards JNK2

a) JIP^{10}-Δ-TAT^{i} is a potent and selective inhibitor towards JNK2, with an IC_{50} ~ 92 nM as determined by fitting the fractional activity at every inhibitor concentration to Morrison's equation for a tight-binding inhibitor (35). b) JIP^{10}-Δ-TAT^{i} exhibits 10-fold greater selectivity for JNK2 compared to JNK1 and JNK3, while maintaining limited potency towards p38MAPKα (150-fold less than JNK2) and ERK2. c) JIP^{10}-Δ-R_9 exhibits an IC_{50} of ~89 nM towards JNK2 (fitting to Morrison's equation (35) for tight-binding inhibitor). d) JIP^{10}-Δ-R_9 exhibits a 10-fold higher selectivity for JNK2 over JNK1 and JNK3 with limited potency towards p38MAPKα and ERK2.

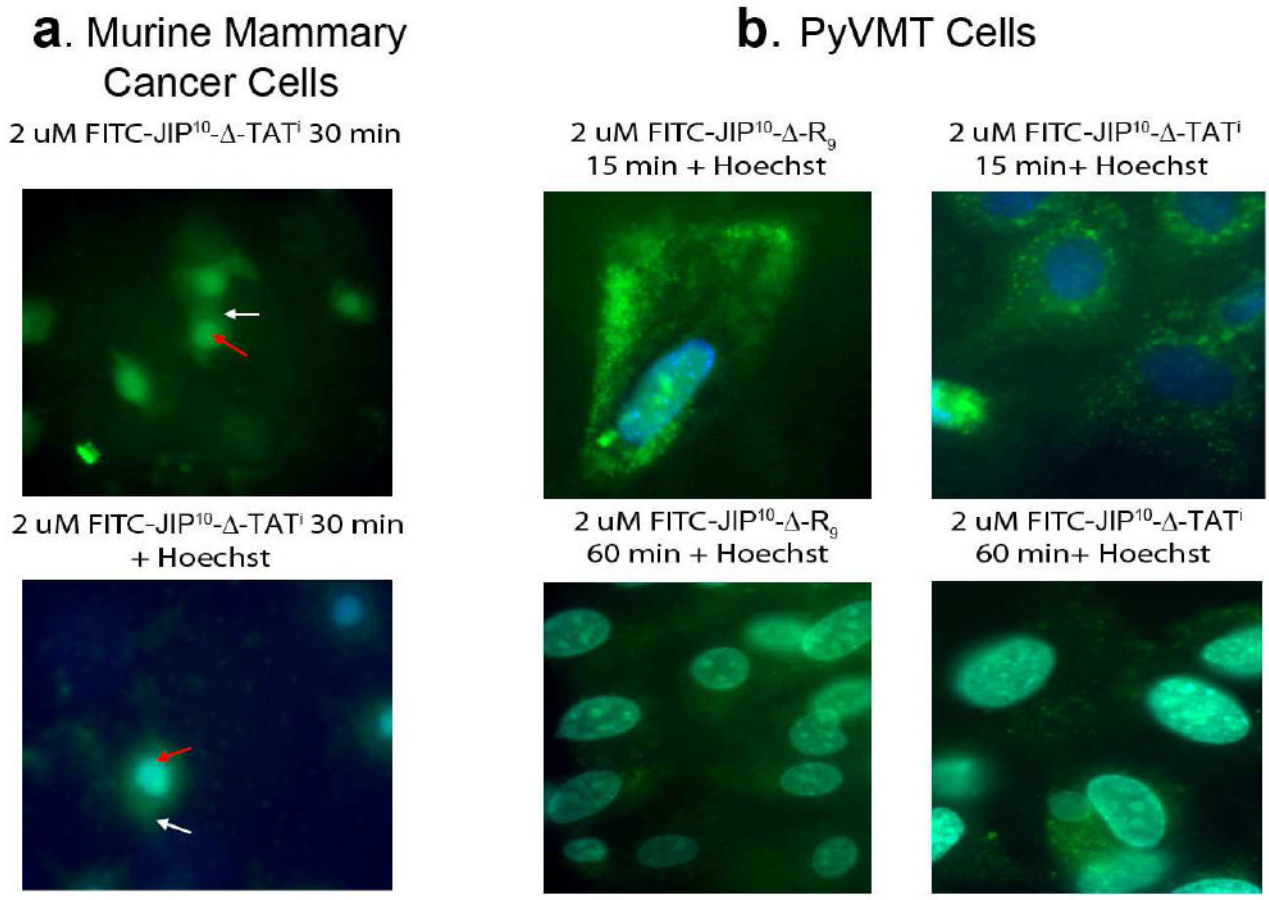

Figure 4. Cellular uptake of JIP peptides

a) Cellular uptake of FITC labeled JIP^{10}-Δ-TAT^{i} was observed as a bright green signal (white arrow for the cytoplasm, red for the nucleus) in 4T1.2 murine mammary carcinoma cells. b) JIP^{10}-Δ-R_9 and JIP^{10}-Δ-TAT^{i} internalization was visualized as robust green punctuates in the cytoplasm of PyVMTjnk2+/+ cells, 15 minutes after addition, and the peptide was retained up to 1 hour post addition. Higher magnification shows relatively higher uptake of JIP^{10}-Δ-R_9 in the early time-point. However, peptide retention was more efficient with the JIP^{10}-Δ-TAT^{i} peptide. Images are representative of data from at least 4 independent experiments.

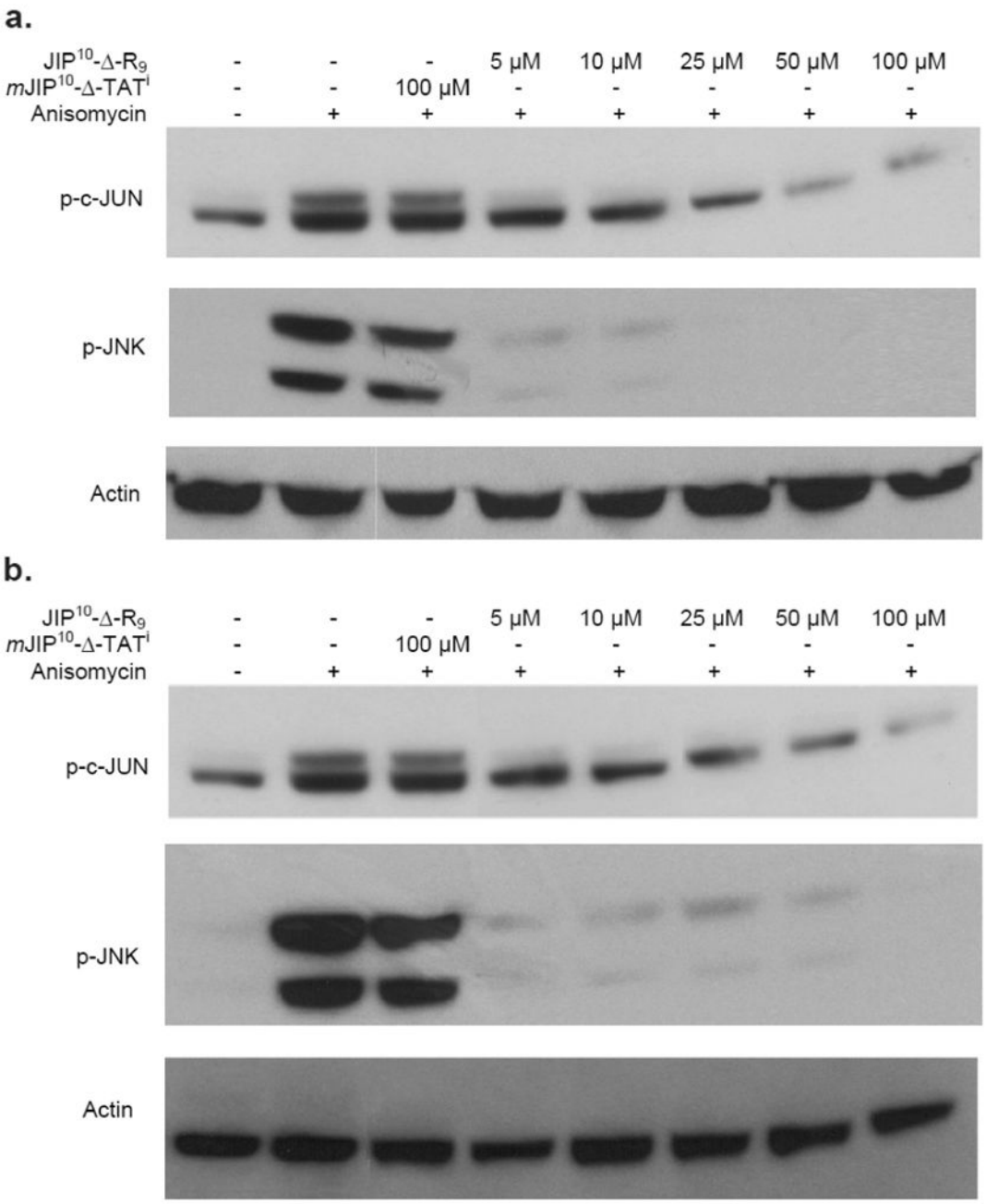

Figure 5. JIP peptides inhibit both JNK activation and c-Jun phosphorylation in HEK293 cells

a) HEK293 cells were treated with JIP^{10}-Δ-R$_9$ (5–100 μM), or *m*JIP^{10}-Δ-TAT^{i} (100 μM) for 16 hours. The JNK pathway was then induced by the addition of anisomycin (50–100 nM) for 5–10 minutes, before lysing the cells. Lysates were fractionated by SDS PAGE (12% gel) and subjected to Western blot analysis in order to detect the phosphorylated forms of c-jun and JNK. b) HEK293 cells were treated with JIP^{10}-Δ-TAT^{i} (5–100 μM), or *m*JIP^{10}-Δ-TAT^{i} (100 μM) and analyzed as in Fig. 5a. These results are representative of two experiments.

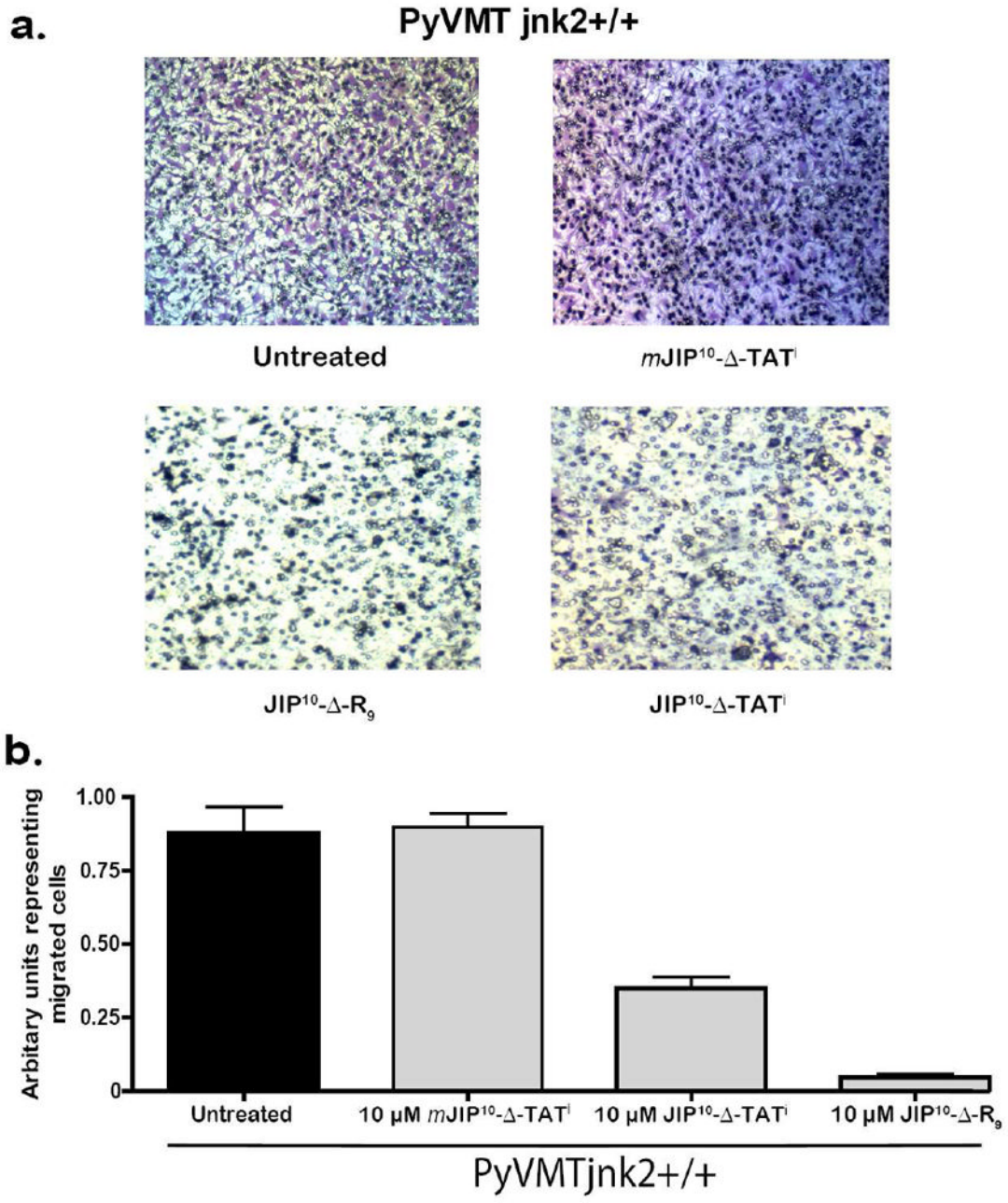

Figure 6. JIP peptides can efficiently inhibit mammary cancer cell migration

a) Representative images of migrated cells on the underside of a transwell membrane stained with crystal violet dye. Untreated PyVMTjnk2+/+ cells migrate similar to cells treated with 10 μM *m*JIP^{10}-Δ-TAT^{i}. 10 μM of JIP^{10}-Δ-R$_9$ and JIP^{10}-Δ-TAT^{i} significantly reduce the number of cells that travel through the transwell pores to successfully reach the underside of the transwell membrane (migrated cells). b) Graphical analysis. Representative of three or more independent experiments. When compared to untreated cells a two-sided Student's t-test analysis gave values of p = 0.84, 0.006 and 0.0008 for cells treated with *m*JIP^{10}-Δ-TAT^{i}, JIP^{10}-Δ-TAT^{i} and JIP^{10}-Δ-R$_9$, respectively.

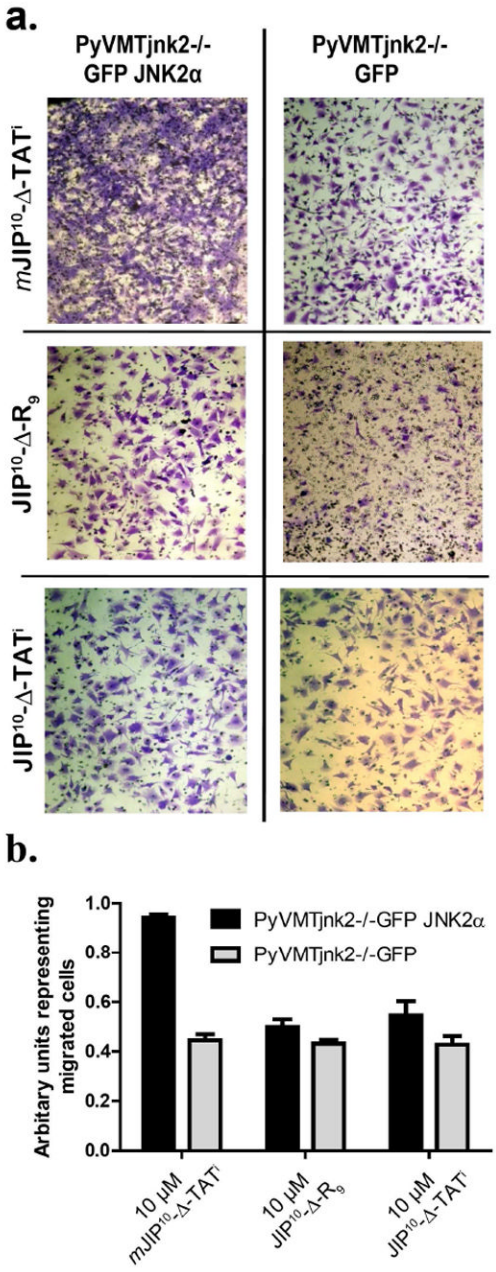

Figure 7. JIP^{10}-Δ-R$_9$ and JIP^{10}-Δ-TAT^{i} specifically target JNK2-mediated cell migration

a) Cell migration assays were performed with various JIP treatments using the isogenic PyVMTjnk2-/-GFP and PyVMTjnk2-/-GFPJNK2 cell lines. Representative fields show migrating cells with normal morphology and cellular extensions. b) Quantification of transwell chamber-based migration assays with *m*JIP^{10}-Δ-TAT^{i}, JIP^{10}-Δ-TAT^{i} or JIP^{10}-Δ-R$_9$ treatment, performed in triplicate using the isogenic PyVMTjnk2-/-GFP and PyVMTjnk2-/-GFPJNK2 lines. Data is representative of at least three independent experiments. Analysis by two-sided Student's t-test comparing the two cell lines gave values of p=0.0001, 0.13, 0.15, when comparing treatments by peptides *m*JIP^{10}-Δ-TAT^{i}, JIP^{10}-Δ-R$_9$ and JIP^{10}-Δ-TAT^{i}, respectively.

Table 1

a. Selectivity of JIP peptides

Peptide	Sequence	JNK1 IC_{50} (μM)[a]	JNK2 IC_{50} (μM)[a]	JNK3 IC_{50} (μM)[a]	p38MAPKα IC_{50} (μM)[a]	ERK2 IC_{50} (μM)[a]
JIP^{10}	Ac-PKRPTTLNLF-amide 10 mer JIP	1±0.05	2±0.15	2.6±0.07	168±4	180±7
TAT-JIP^{10}	Ac-YGRKKRRQRRR-RPKRPTTLNLF-amide TAT-11 mer JIP	1.1±0.1	1.8±0.2	1.9±0.18	–	–
TAT-*pp*-JIP^{20}	Ac-GRKKRRQRRR-**PP**-RPKRPTTLNLFPQVPRSQDT-amide TAT-*bi*proline linker-20 mer JIP	0.33±0.01	0.45±0.04	**0.06±0.005**	1.45±0.1	179±18
JIP^{10}-Δ-TAT^{i}	Ac-PKRPTTLNLF-**AHX**-RRRQRRKKRG-amide[b] 10 mer JIP-AHX Linker-Inverse TAT	1.16±0.05	**0.092±0.003**	1.2±0.07	13.7±2.9	161±8
JIP^{10}-Δ-R_9	Ac-PKRPTTLNLF-**AHX**-RRRRRRRRR-amide 10 mer JIP-AHX Linker- Poly Arginine	1.1±0.13	**0.089±0.005**	1.2±0.09	14.1±1.4	206±5.8
mJIP^{10}-Δ-TAT^{i}	Ac-PKRPTT**R**NLF-**AHX**-RRRQRRKKRG-amide 10 mer JIP Arg mutant-AHX Linker-Inverse TAT	1900±37	420±30	900±81	447±14	580±30
b. Selectivity of *retro-inverso* JIP peptides						
Peptide	Sequence	JNK1 IC_{50} (μM)[a]	JNK2 IC_{50} (μM)[a]	JNK3 IC_{50} (μM)[a]	p38MAPKα IC_{50} (μM)[a]	ERK2 IC_{50} (μM)[a]
D-JIP^{10}	Ac-FLNLTTPRKP-amide Retro-inverso JIP^{10}	5900±307	2500±171	1800±95	1000±79	
D-JIP^{20}	Ac -TDQSRPVQPFLNLTTPRKPR-amide Retro-inverso JIP^{20}	2200±25	1500±109	415±28	1400±149	
D-TAT-*pp*-JIP^{20}	Ac-TDQSRPVQPFLNLTTPRKPR-**PP**-RRRQRRKKRG-amide Retro-inverso of JIP^{10}-Δ-TAT^{i}	288±24	355±79	76.3±6.8	**1.87±0.18**	206±37

[a] IC50 Determined as described in Methods section.

[b] Δ: aminohexanoyl.

D: *retro-inverso*